THE JOURNAL OF BIOLOGICAL CHEMISTRY VOL. 281, NO. 49, pp. 37486–37495, December 8, 2006

The Basic Domain of TRF2 Directs Binding to DNA Junctions Irrespective of the Presence of TTAGGG Repeats*

Received for publication, September 11, 2006, and in revised form, October 18, 2006 Published, JBC Papers in Press, October 18, 2006, DOI 10.1074/jbc.M608778200

Nicole Fouché[‡], Anthony J. Cesare[§], Smaranda Willcox[‡], Sezgin Özgür[‡], Sarah A. Compton[‡], and Jack D. Griffith[‡1]

From the [‡]Lineberger Comprehensive Cancer Center and Department of Biochemistry and Biophysics, University of North Carolina, Chapel Hill, North Carolina 27599 and [§]Cancer Research Unit, Children's Medical Research Institute, Westmead, New South Wales 2145, Australia

The replication of long tracts of telomeric repeats may require specific factors to avoid fork regression (Fouché, N., Özgür, S., Roy, D., and Griffith, J. (2006) *Nucleic Acids Res.*, in press). Here we show that TRF2 binds to model replication forks and four-way junctions *in vitro* in a structure-specific but sequence-independent manner. A synthetic peptide encompassing the TRF2 basic domain also binds to DNA four-way junctions, whereas the TRF2 truncation mutant (TRF2$^{\Delta B}$) and a mutant basic domain peptide do not. In the absence of the basic domain, the ability of TRF2 to localize to model telomere ends and facilitate t-loop formation *in vitro* is diminished. We propose that TRF2 plays a key role during telomere replication in binding chickenfoot intermediates of telomere replication fork regression. Junction-specific binding would also allow TRF2 to stabilize a strand invasion structure that is thought to exist at the strand invasion site of the t-loop.

Telomeres are nucleoprotein structures that protect the ends of chromosomes and are essential for regulating the replicative lifespan of somatic cells. The DNA component of the mammalian telomere consists of long double-stranded (ds)[2] tracts of the hexameric repeat unit TTAGGG (2) that ends with a G-rich 3′ single-stranded (ss) overhang (3). Telomeric DNA is thought to be organized into a t-loop "end-capping" structure by the telomere-binding proteins TRF1, TRF2, and POT1 and the proteins that bind to them, TIN2, TPP1, and Rap1 (4, 5). This higher order structure may enable cells to distinguish chromosome ends from random double-strand breaks. Large blocks of telomere repeat sequences can be lost when these end-capping proteins are disrupted, or problems are encountered during DNA replication or repair (for review, see Ref. 6). This typically results in p53- and Rb-mediated senescence or cellular crisis, as evidenced by end-to-end fusions of chromosomes, ATM-dependent activation of p53, and apoptosis (for review, see Ref. 7).

Much has been learned about the properties of TRF1 and TRF2 including their binding to DNA and the effects of their ablation or overexpression in the cell. We observed that TRF1 forms filamentous structures on long tracts of telomeric DNA *in vitro* (8), whereas TRF2 binds preferentially to the telomeric DNA at the junction between the duplex repeats and the ss overhang (9). Both TRF1 and TRF2 contain a similar Myb domain at their COOH terminus that mediates their binding to ds telomeric DNA (10). TRF1 and TRF2 differ in their NH_2 termini, however, which are rich in either acidic residues in TRF1 or basic residues in TRF2. The function of the basic domain of TRF2 is poorly understood. Deletion of this domain (TRF2$^{\Delta B}$) does not impede the DNA binding activity of TRF2 or its localization to telomeres *in vivo*, but expression of TRF2$^{\Delta B}$ resulted in stochastic deletions of telomeric DNA, generation of t-loop-sized telomeric circles, cell cycle arrest, and induction of senescence in human cells (11, 12). In addition, recent evidence suggested that the basic domain, but not the Myb domain, was required for TRF2 association with photo-induced double-strand breaks in non-telomeric DNA in human fibroblasts (13).

Relatively little is known about the replication of mammalian telomeric DNA *in vivo*; however, experiments in ciliates and budding yeast have provided insight into how this occurs in other eukaryotes. During each round of replication, all but the very end of the telomere is replicated by the conventional semi conservative polymerase machinery (14). Leading strand sequences eroded in the last round of replication (end replication problem) can be restored by the reverse transcriptase telomerase (15), whereas the lagging strand is concurrently elongated by polymerases α and δ using the newly formed G strand as the template (16).

A possible complication of replication at the telomere is the requirement for protecting the DNA ends from recognition by DNA repair factors while still allowing the DNA to be accessible to the replication machinery. Also, replication of telomeric DNA tends to stall *in vitro* (17), and long blocks of telomeric repeats are highly unstable when transformed into *Escherichia coli* cells that lack recombination enzymes, suggesting difficulties with DNA replication through the telomeric tract.[3] Furthermore, the G-rich strand of telomeric DNA has the tendency to form G-quartets (18), and the complementary cytosine-rich strand can fold into an intercalated tetramer called the i-motif (19).

* This work was supported in part by the Ellison Medical Foundation and National Institutes of Health Grants GM31819 and ES013773 (to J. D. G.). The costs of publication of this article were defrayed in part by the payment of page charges. This article must therefore be hereby marked "*advertisement*" in accordance with 18 U.S.C. Section 1734 solely to indicate this fact.

[1] To whom correspondence should be addressed. Tel.: 919-966-2151; Fax: 919-966-3015; E-mail: jdg@med.unc.edu.

[2] The abbreviations used are: ds, double-stranded; ss, single-stranded; EM, electron microscopy; TRF2$^{\Delta B}$, TRF2 basic domain truncation mutant; aa, amino acid(s); WRN, Werner syndrome helicase; BLM, Bloom syndrome helicase.

[3] N. Fouché, unpublished data.

The fact that human telomeres are replicated as rapidly as the bulk DNA (20) suggests that in addition to the standard replicative machinery, telomere-targeted factors may exist to actively facilitate its rapid replication. Direct evidence for the requirement of such telomeric factors at the replication fork was recently discovered in the fission yeast *Schizosaccharomyces pombe*, where the telomere-binding protein Taz1 is required for efficient replication of telomeres (21). Also, in addition to the normal replicative helicases present at forks, the RecQ helicases WRN and BLM, implicated in premature aging diseases, have been shown to be important for proper telomere replication and maintenance in human cells (22–24).

The RecQ helicases have been shown to unwind G quartets (25) and promote branch migration of four-stranded junctions similar to chickenfoot structures (26, 27). In human cells TRF2 co-localizes and physically interacts with WRN (28), and it binds to and stimulates the activities of both the WRN and BLM helicases *in vitro* (29). TRF1 and POT1 have also been shown to regulate WRN and BLM unwinding of telomeric substrates *in vitro* (30, 31). Furthermore, *in vitro* overexpression of TRF1 and TRF2 led directly to replication fork stalling (17), suggesting that the telomere binding factors also have a direct effect on the replication machinery.

We recently discovered a new feature of telomeric DNA that may explain this requirement for the RecQ helicases during telomere replication. Using electron microscopy (EM) and model replication fork templates that mimic a replication fork that had transited a long block of telomeric repeats, we discovered that telomeric DNA is inherently more slippery than non-repeat-containing DNA, such that the replication forks are able to more easily transition back and forth between non-regressed and fully regressed states (1). During replication, repeat-containing DNA could, therefore, spend a significantly larger fraction of time in the partially regressed state, characterized by a Holliday junction or "chickenfoot" structure, than other DNAs. We believe that this presents a significant problem to the cell, where these four-stranded structures could result in recruitment of unwanted recombination factors or lead to deleterious recombination events if repaired. p53 will also bind to stalled chickenfoot structures with great affinity, suggesting that it may have the ability to halt excessive fork regression (32). These observations led us to ask whether one or both of the primary ds telomere-binding proteins TRF1 and TRF2 might also show some unusual binding with regard to three- and four-way DNA junctions when they occur within telomeric tracts.

To test this hypothesis we generated a set of DNA templates including telomeric and non-telomeric replication forks, Holliday junctions, and model telomeres containing 3′ overhangs. Using EM and polyacrylamide gel-shift assays, we evaluated binding to these templates by TRF1, TRF2, and TRF2$^{\Delta B}$ as well as a peptide encompassing the basic domain of TRF2 and another similar "mutant" peptide containing a rearrangement of four amino acids (aa).

In this paper we show that TRF2, but not TRF1 or TRF2$^{\Delta B}$, is able to target the junctions of replication forks, chickenfoot structures, and Holliday junctions. Junction binding occurred irrespective of the presence of TTAGGG repeats, and a bias for four-stranded junctions was detected. The peptide mimicking the basic domain of TRF2 recapitulated this four-way junction binding, whereas the mutant peptide could not. Furthermore, in the absence of other telomere-binding proteins, TRF2 lacking the basic domain had a reduced ability to target the end of the large model telomeres and facilitate t-loop formation *in vitro*. We, therefore, suggest a novel role for the previously uncharacterized basic domain of TRF2, which is to facilitate TRF2 binding to chickenfoot intermediates of telomere replication fork regression, presumably preventing their recognition by Holliday junction resolvases. The data are also the first direct demonstration of TRF2 binding to DNA junctions, irrespective of the presence of telomeric repeats.

EXPERIMENTAL PROCEDURES

DNA Probes and Templates—[γ-^{32}P]ATP end-labeled J12 four-way junction probes (33), large Holliday-junction DNA templates (HJ575 (34)), model non-telomeric replication forks (32), and model telomere DNA (9) were synthesized as previously described. A telomeric probe with a 14-nucleotide overhang was prepared by annealing the [γ-^{32}P]ATP end-labeled oligonucleotide (oligo) 5′-CTAACCCTAACCCTGTCCTAGCAATGTAATCGTCTATGAGTCTG-3′ to the oligo 5′-CAGACTCATAGACGATTACATTGCTAGGACAGGGTTAGGGTTAGGGTTAGGGTTAGGG-3′. A hairpin probe consisting of a 7-nucleotide linker and a 21-bp stem was prepared by heating and stepwise cooling the [γ-^{32}P]ATP end-labeled oligo 5′-CTTATTCACAGACCACGACTCAAAAAAAGAGTCGTGGTCTGTGAATAAG-3′. All annealed products were purified on 10% nondenaturing polyacrylamide gels.

Telomeric replication forks were created using a variant of pRST5 (9) containing a nicking site directly adjacent to the telomeric repeat tract (1). The plasmid was nicked with N.BbvC IA (New England Biolabs, Ipswich, MA) and then incubated with the Klenow fragment (exo$^-$) of DNA polymerase 1 (New England Biolabs) and 0.5 mM each of dTTP, dATP, and dGTP to generate an ss tail by strand displacement of the repeat tract. The ss tail was converted to a ds tail by annealing a 228-fold molar excess of the oligo 5′-CCCTAACCCTAACCCTAACCCTAA-3′ to the template for 30 min at 37 °C in 100 mM NaCl and ligating with T4 DNA ligase (400 units, New England Biolabs) at 16 °C overnight in 50 mM NaCl, 10 mM Tris-HCl (pH 7.9), and 1 mM dithiothreitol. When required, the replication templates were linearized with XmnI (New England Biolabs) for 1 h at 37 °C.

Proteins and Peptides—NH_2-terminal His_6-tagged human TRF1, TRF2, and TRF2$^{\Delta B}$ were purified to homogeneity from baculovirus-infected insect cells by the method of Bianchi *et al.* (35) except that a Talon™ metal affinity resin (Clontech, Palo Alto, CA) was employed instead of nickel-nitrilotriacetic acid (35). p53 as well as the carboxyl-terminal domain of the p53 protein comprising amino acid residues 311–393 were purified as previously described (36).

Two peptides, each containing an NH_2-terminal biotin motif, were synthesized by the UNC Micro-Protein Facility, University of North Carolina School of Medicine, Chapel Hill, NC (Fig. 1*B*). The first peptide (Peptide_B) consisted of aa 2–31 of wild type human TRF2 (10), whereas the second peptide

(Peptide_M) comprised a 4-aa sequence rearrangement of the first peptide.

Electron Microscopy—Binding assays of TRF2 and TRF2$^{\Delta B}$ to the model telomere were done as previously described (9). Complexes of p53, TRF1, TRF2, TRF2$^{\Delta B}$, and both peptides with Holliday junction or replication fork DNA were formed by incubating a 25:1 molar ratio of protein monomer:DNA in a 20-μl volume of EM buffer (20 mM HEPES (pH 7.5), 0.1 mM EDTA, 0.5 mM dithiothreitol, 75 mM KCl) for 20 min at room temperature. A 5× molar excess of streptavidin (Molecular Probes, Eugene, OR) to peptide was added to samples containing biotin-tagged peptide for 5 min at room temperature. Samples were fixed with 0.6% (w/v) glutaraldehyde for 5 min at room temperature followed by filtration through 2-ml columns of 2% agarose beads (50–150 μm, Agarose Bead Technologies, Tampa, FL) pre-equilibrated with 0.01 M Tris-HCl (pH 7.6), 0.1 mM EDTA. The purified samples were prepared for EM by rotary shadow-casting with tungsten as previously described (37). An FEI Tecnai 12 electron microscope equipped with a Gatan ultrascan camera (model US4000SP) were used to photograph images.

Mobility Shift Assays—Reaction mixtures (10 μl) containing probes (10 nM) and the proteins (see legends to Figs. 3 and 5 for details) were incubated at room temperature for 20 min in EM buffer. The mixtures were adjusted to 10% glycerol and loaded on 3.5% non-denaturing polyacrylamide gels in 45 mM Tris borate, 1 mM EDTA. The gels were run at 140 V for 1 h at 4 °C, dried, analyzed by autoradiography, and quantified using a Storm 840 PhosphorImager (GE Healthcare).

Calculating K_d—GraphPad Prism (GraphPad Software, Inc., San Diego, CA) was used for nonlinear regression of the data obtained from the mobility shift assays. The one-site hyperbolic binding equation used was % probe shifted = (B_{max} × [nM protein])/([nM protein] + K_d). In experiments with the Holliday junction probe, dissociation constant (K_d) values were converted to association constant (K_a) values ($K_a = 1/K_d$) then multiplied by the EM-specific binding factor (see "Results") ($K_{a,apparent} = K_a \times$ % EM junction binding) and again converted to a dissociation constant ($K_{d,apparent} = 1/K_{a,apparent}$ (nM)).

RESULTS

To examine the binding of TRF1 and TRF2 to replication forks and Holliday junctions and to compare this with previous studies of p53 (32), a series of large model templates were constructed for EM. Previously we described the generation of a model replication fork consisting of an ~500-bp arm extended from a 3-kilobase linear or circular DNA at a unique site, which is at the end of a 500-bp cassette consisting of a random but G-less sequence (32). We constructed a new replication fork template based on this design from a plasmid containing a 560-bp telomeric cassette (Fig. 1*A*). In this DNA two arms of the Y-fork molecule contain telomere repeats leading up to the fork junction. In addition, a Holliday junction template containing 500-bp arms of plasmid-derived DNA extended from the well known J12 junction was prepared as previously described (33).

Purified TRF1 and TRF2 were incubated with the template DNAs and prepared for EM. EM binding experiments were conducted in parallel with purified p53. For these studies p53

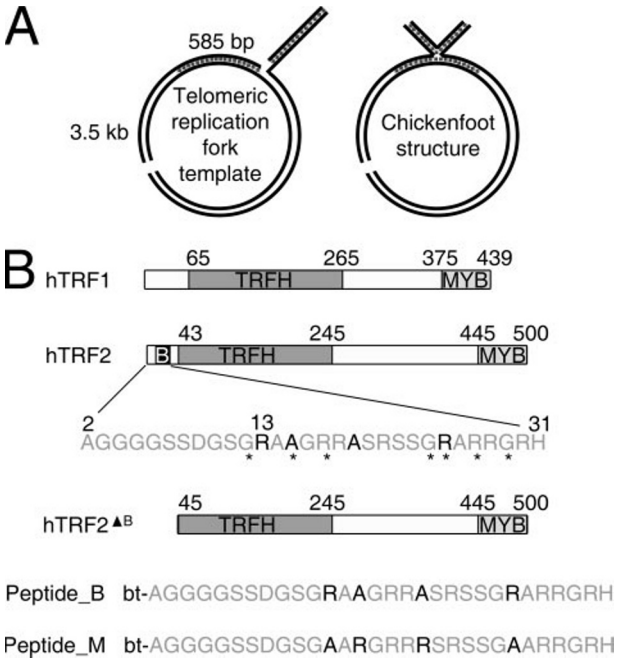

FIGURE 1. **DNA, protein, and peptide constructs used in this study.** *A*, telomeric replication fork template and chickenfoot structure; the *patterned region* indicates TTAGGG repeats. *B*, TRF1 and TRF2 have similar TRF homodimerization (TRFH) and Myb DNA-binding domains. TRF2 has a unique NH_2-terminal basic domain (*B*, aa 13–30) with conserved residues (indicated by an *asterisk*). TRF2$^{\Delta B}$ is a deletion mutant of TRF2 lacking the first 44 aa. The basic (Peptide_B) and mutant (Peptide_M) peptides have an NH_2-terminal biotin moiety (*bt*), and they differ in their sequences (*gray lettering*) by a re-arrangement of four aa (*black lettering*). *hTRF*, human TRF.

was chosen for comparison with TRF2 not in an effort to argue for the biological relevance if its binding to replication forks or Holliday junctions but, rather, that it is of similar size to TRF2, it binds these junctions tightly without altering their structure significantly, and we have on hand data of p53 binding to the very DNA templates used in this study. Examination of fields of molecules from incubations of TRF2 with the model telomere replication fork revealed several DNA-protein configurations. When a 25:1 molar ratio of TRF2 monomers to DNA template was used, approximately one-third of all molecules contained a particle of TRF2 bound at the center of the stalled fork junction (Fig. 2*A*). Of these molecules, a subset of the forks had regressed, generating chickenfoot structures, and TRF2 was also observed bound at these junctions (*inset*, Fig. 2*A*). The remainder of the DNA consisted of DNA templates with no protein bound (the majority), a fewer number of DNAs containing TRF2 protein bound elsewhere on the DNA template but not at the fork junction, and more frequently, aggregates of two or more DNAs bound by a large mass of TRF2 (data not shown). These aggregates became more abundant in binding preparations containing molar ratios of TRF2 monomers to DNA template greater than 25:1. Of the TRF2-bound molecules where TRF2 was not located at the fork junction, the majority had TRF2 bound sufficiently close to the fork that we presumed it was bound along the TTAGGG tracts. Quantification of the results from scoring hundreds of molecules is described below. Although the TRF2 particles varied in size, in most cases the size range was much less variable when bound to the center of the three- or four-way junction than in the

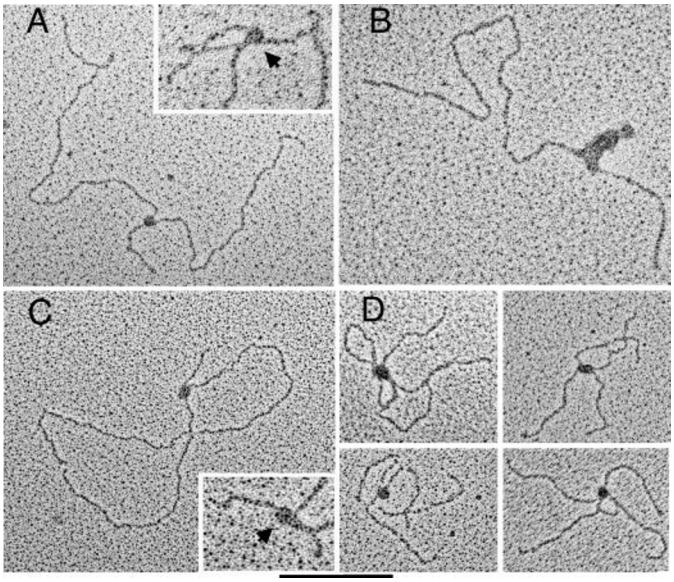

FIGURE 2. **TRF2 binds DNA junctions *in vitro*.** *A* and *C*, discrete complexes of TRF2 bound to the junctions of the three-stranded replication forks and the four-stranded chickenfoot structures (*arrow*, *inset*) (*A,* telomeric template; *C*, non-telomeric template). *B*, extensive, filamentous binding of TRF1 to a model telomeric replication forks. *D*, TRF2 bound to the center of Holliday junction template DNAs. The *bar* is equivalent to 450 bp in the panels showing full-length molecules.

instances when TRF2 was observed bound along the duplex TTAGGG tracts (Fig. 2*A*, *inset*), and the particle size was suggestive of TRF2 dimers or tetramers. When parallel experiments were performed with TRF1, the telomeric repeats were complexed by multiple protein particles (Fig. 2*B*) resembling the TRF1 filaments formed along duplex TTAGGG tracts as previously described (8).

For comparison, TRF1 and TRF2 were incubated with the random sequence replication fork template lacking TTAGGG repeats. The binding of TRF1 to this template was low (quantified in Fig. 3*A*), as expected from the lack of telomeric repeats. Of great interest, however, was the observation that incubation of TRF2 with this template led to discrete TRF2 complexes at the three- or four-way junctions (Fig. 2*C*). In molecules in which the forks had regressed into four-way chickenfoot forms, TRF2 complexes were more frequently observed bound to the DNA and almost always at the four-way junction (*inset*, Fig. 2*C* and quantified below). This led us to examine TRF2 binding to Holliday junction DNA containing 500-bp arms (Fig. 2*D*). Indeed, by EM we found that TRF2 bound well to these structures, localizing to the center of the four-way junction. By comparison, TRF1 bound less well to these structures, and when it did, the binding appeared to be random (quantified in Fig. 3*B*).

We previously examined the binding of p53 to random sequence replication fork templates (32) as well as to large Holliday junction templates (33). We were, thus, able to combine these results in a comparison of TRF1 and TRF2 binding to these templates (Fig. 3, *A–C*). An average of 179 molecules over three experiments was counted per experimental condition.

Incubation of p53 (25:1) with the telomeric replication fork template resulted in observation of p53 at the fork and the frequency (69 ± 3 *versus* 8 ± 1% elsewhere on the DNA; Fig. 3*A*) was comparable with previous observations with non-telomeric forks (56% at the fork *versus* 15% bound elsewhere (32)). We could not assess TRF1 binding to telomeric replication fork templates because of its extensive binding to the telomeric tract. Also, because the number of DNA molecules contained within the TRF2 aggregates could not be determined by EM, they were not included in the total number of DNAs counted. Thus, the actual level of TRF2 binding to the telomeric replication fork is likely to be higher than the value cited here (34 ± 21 *versus* 6 ± 2% elsewhere on the DNA; Fig. 3*A*) because the values were calculated as the percentage of the individual (non-aggregated) DNAs only. The relatively wide spread in calculated TRF2 binding is most likely due to a variation in the abundance of TRF2 aggregates in these samples, because when TRF2 binding in these samples was evaluated as a percentage of individually bound molecules, the S.D. was small (76 ± 5% bound at the junction *versus* 24 ± 5% bound elsewhere).

A greater bias for the DNA junction was revealed for TRF2 binding to non-telomeric replication forks, where protein-DNA aggregates were less abundant, and TRF2 bound to the fork junction 48 ± 6% of the time and elsewhere on the DNA only 5 ± 3% of the time. This was in contrast to TRF1 binding to the non-telomeric replication forks, which was lower and seemingly random; only 6 ± 1% of molecules had TRF1 bound at the fork junction, whereas 13 ± 5% had TRF1 bound somewhere else on the DNA.

TRF2 bound well to the Holliday junction templates, targeting the center of the 4-way junctions 75 ± 5% of the time and binding elsewhere on the DNA only 8 ± 4% of the time (Fig. 3*B*). Previously, when p53 binding to Holliday junctions was studied by EM, 59% of all molecules were bound at their center by p53 (33). When TRF1 binding to the Holliday junction templates was examined, we found that it bound less well (18 ± 6% bound at the junction) than TRF2 and that most binding occurred on one or more of the arms of the Holliday junction rather than at the DNA junction (27 ± 5%).

When binding to non-telomeric replication forks was examined in more detail it became apparent that TRF2 has a greater affinity for the four-stranded replication fork structures (Fig. 3*C*). Specifically, we considered TRF2 binding to the Y-shaped three-way junctions as a fraction of all three-stranded junctions and, similarly, TRF2 binding to the chickenfoot four-way junctions as a fraction of all four-way junctions. A bias was observed where TRF2 bound to 89 ± 4% of all 4-way junctions *versus* 36 ± 11% of all 3-way junctions. When the DNA template contained telomeric repeats, this preference was not as obvious (42 ± 3% of all 4-way junctions *versus* 13 ± 4% of all 3-way junctions), suggesting that the sequence-specific binding of TRF2 to the surrounding sequences led to the apparent lower fractional localization to the fork. p53 showed a smaller bias for chickenfoot structures when bound to the telomeric replication fork (82 ± 1% of all 4-way junctions *versus* 59 ± 10% of all 3-way junctions) and no bias when binding to non-telomeric replication forks (~52 ± 8% of all 4-way junctions *versus* 52 ± 7% of all 3-way junctions (32)). Collectively, these data suggest, therefore, that TRF2 has an affinity for DNA junctions, with a bias for four-stranded DNA junctions resembling Holliday junctions.

To further examine the binding of these proteins to fork junctions, mobility shift assays were carried out using TRF2,

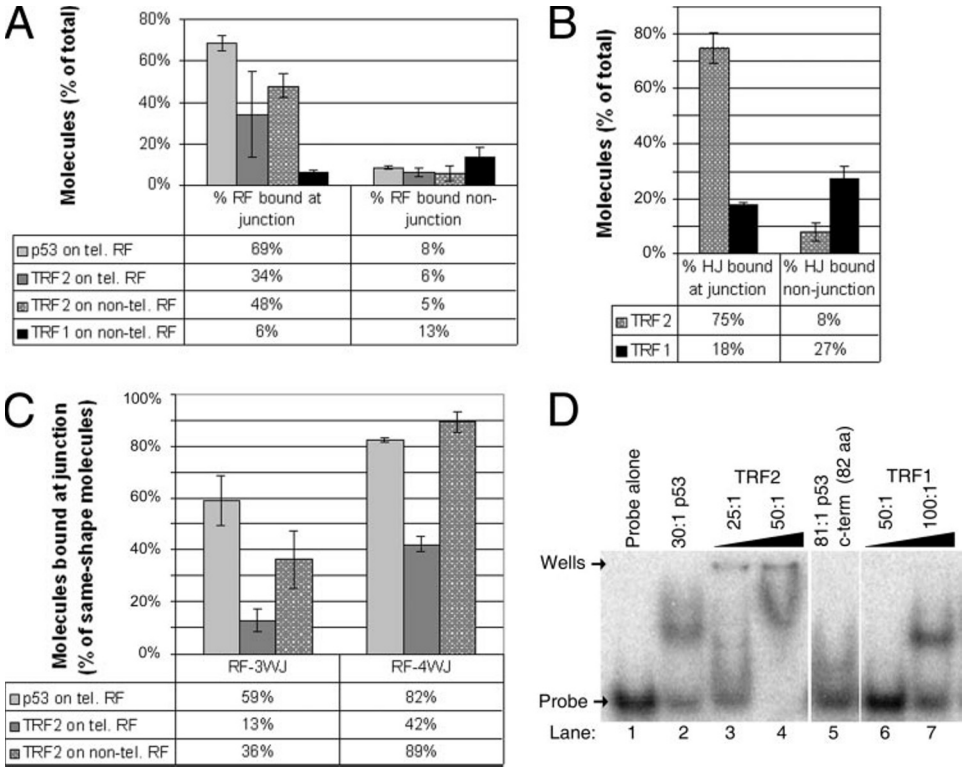

FIGURE 3. **TRF2 junction binding is biased toward four-way junctions.** *A*, binding of p53, TRF2, and TRF1 to the telomeric replication fork templates (*tel. RF*) and the non-telomeric replication fork templates (*non-tel. RF*) was visualized by EM and quantified. Percentages are calculated as a fraction of all replication forks counted (three-way and four-way junctions combined). Only molecules with protein bound at the junction of the replication fork or chickenfoot structure were considered junction-bound molecules. Data are represented as the mean ± S.D. *B*, Holliday junction (*HJ*) templates bound by TRF1 or TRF2 were similarly quantified. *C*, percentages of TRF2 and p53 binding to replication forks are calculated as a fraction of molecules with the same shape. *D*, mobility shift assay of the γ-^{32}P-labeled J12 junction probe alone (*lane 1*) or bound by p53 (at a molar ratio of 30:1 protein:probe, *lane 2*), TRF2 (25:1, *lane 3*; 50:1, *lane 4*), an 82-aa COOH-terminal fragment of p53 containing the basic domain (81:1, *lane 5*), and TRF1 (50:1, *lane 6*; 101:1, *lane 7*).

TRF1, p53, and the 82-aa COOH-terminal fragment of p53 with a 100-bp γ-^{32}P end-labeled Holliday junction probe (Fig. 3*D*). TRF2 shifted the Holliday junction probe equally as well as p53, confirming our EM results. In contrast, approximately four times as much TRF1 was required to observe any shift of the probe, suggesting that this interaction with the Holliday junction probe may be nonspecific for the DNA strands (as was visualized by EM). As a control, we duplicated these binding assays with a small γ-^{32}P end-labeled hairpin probe, and in this case neither TRF1 nor TRF2 was able to bind to and shift the probe (data not shown).

These results suggest that TRF2 and p53 share common features in binding to three-way and in particular four-way junctions in a non-sequence-specific manner. This activity resides in the COOH-terminal basic domain of p53. To determine whether the basic domain of TRF2 is involved in targeting TRF2 to DNA junctions, we purified an NH_2-terminal deletion mutant of TRF2 lacking the TRF2-specific basic domain (TRF2$^{\Delta B}$, Fig. 1*B*). We also had a peptide synthesized (Peptide_B, Fig. 1*B*) that consisted of the amino acid sequence from aa 2–31 of TRF2 and, thus, encompassed the basic domain (aa 13–31) of TRF2. In addition, we had a mutant peptide synthesized (Peptide_M, Fig. 1*B*) comprising the same number and composition of amino acids as Peptide_B such that the overall positive charge of both peptides was the same but containing a rearrangement of four amino acids, two of which were conserved among the species *Gallus gallus* (Chicken), *Muntiacus reevesi* (Chinese muntjak), *Muntiacus muntjak vaginalis* (Muntjak), *Mus musculus* (Mouse), and *Homo sapiens* (human) (homologous vertebrate genes data base, HOVERGEN).

EM binding experiments were conducted with these proteins using the same conditions as used for TRF2 and TRF1, except that streptavidin was added to each of the peptide-containing samples just before sample preparation for EM. Both peptides contained an NH_2-terminal biotin moiety to which streptavidin could bind, thereby increasing the overall molecular weight of the peptides from 3 to 56 kDa (equivalent to a monomer of TRF2 of 55 kDa) and allowing them to be visualized by EM.

In experiments examining TRF2$^{\Delta B}$ binding to telomeric replication fork templates, the large majority of molecules consisted of aggregates of two or more DNAs bound by a large mass of TRF2$^{\Delta B}$ protein, although in some cases individual molecules of DNA could be seen. Frequently, these individual DNAs contained long arrays or masses of bound TRF2$^{\Delta B}$, although less often we were able to visualize a discrete particle of TRF2$^{\Delta B}$ bound to the DNA (Fig. 4*A*). In such instances, TRF2$^{\Delta B}$ was localized to the telomeric repeats (on the displaced strand or within a distance equivalent to 500 bp from the fork junction), but it was rarely observed bound to the replication fork junction. We, therefore, conclude that the TRF2$^{\Delta B}$ protein does not show a preference for binding to telomeric replication fork junctions rather binding to the telomeric repeats in a manner similar to TRF1. However, we cannot rule out that the aggregates of TRF2$^{\Delta B}$ that bound to two or more DNAs also included junction-bound molecules or that this complicated pattern of binding reflects a different mode of binding to the DNA junctions rather than the absence of binding. Nevertheless, because most of the TRF2$^{\Delta B}$ protein in the sample was contained within the aggregates of TRF2$^{\Delta B}$, we were not able to quantify TRF2$^{\Delta B}$ binding to this template DNA.

We did not separately quantify binding of the peptides to the telomeric replication fork templates. The peptides do not have a telomere-repeat recognition motif and were observed to have similar binding to these templates (Fig. 4*B*) as to the non-telomeric replication fork templates (Fig. 4*C*). In experiments containing Peptide_B and the non-telomeric replication fork template, 41 ± 1% of all molecules consisted of a complex of streptavidin and Peptide_B bound at the center of the stalled

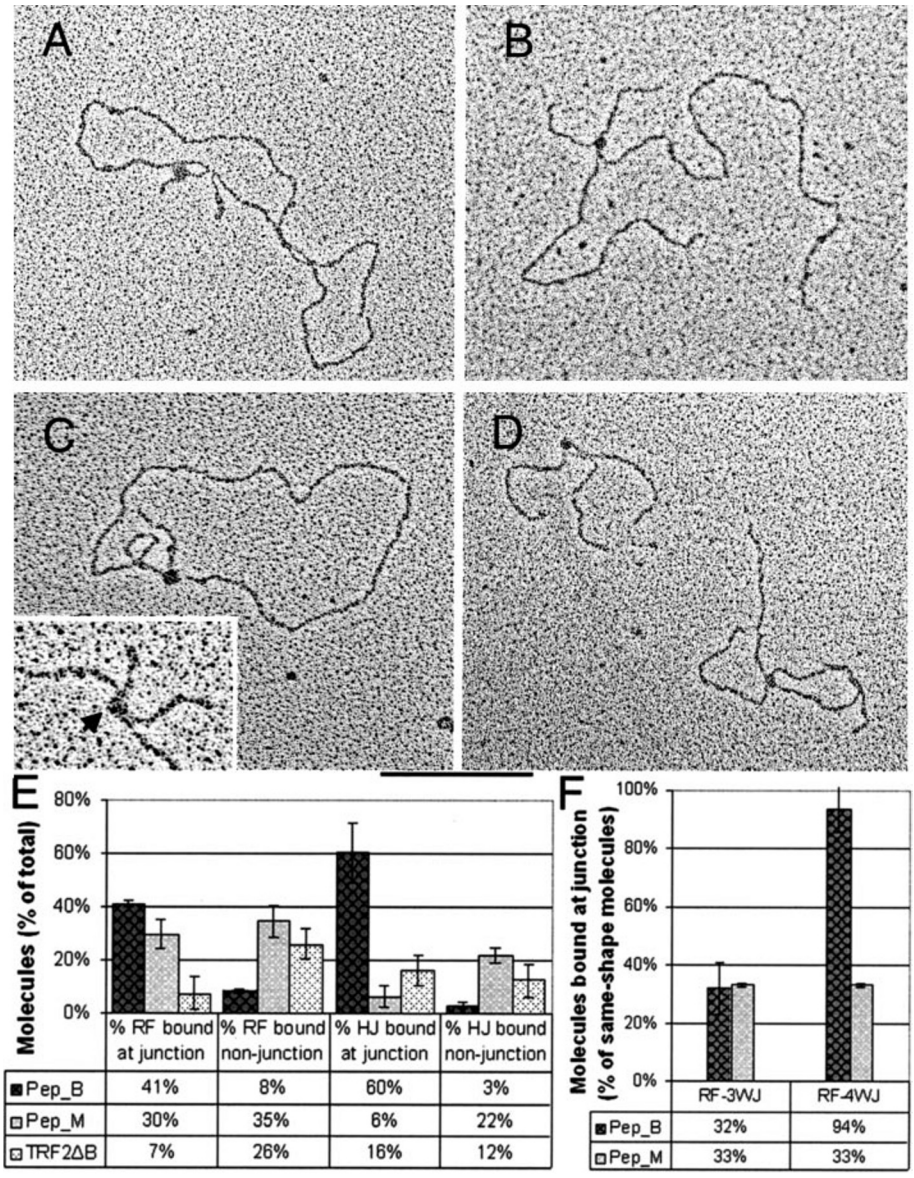

FIGURE 4. **The TRF2 basic terminus binds DNA junctions *in vitro*, whereas TRF2$^{\Delta B}$ protein does not.** *A*, TRF2$^{\Delta B}$ bound to the TTAGGG repeats of the telomeric replication fork template. *B–D*, discrete molecules of streptavidin-bound Peptide_B at the junctions of the telomeric chickenfoot structure (*A*), the non-telomeric replication fork (*C*) or chickenfoot structure (*arrow*, *inset*), and the Holliday junction template DNAs (*D*). The *bar* is equivalent to 450 bp in the panels showing full-length molecules. *E*, binding of the TRF2 basic peptide (Pep_B), the mutant peptide (Pep_M), and TRF2$^{\Delta B}$ to the non-telomeric replication fork templates (*RF*), and the Holliday junction templates (*HJ*) was visualized by EM and quantified. Percentages are calculated as a fraction of all molecules counted. Only molecules with protein bound at the replication fork junction or at the center of the four strands of the Holliday junction were considered junction-bound molecules. *F*, percentages of the basic peptide (Pep_B) and the mutant peptide (Pep_M) binding to non-telomeric replication forks are calculated as a fraction of molecules with the same shape. *RF-3WJ*, 3-way junctions; *RF-4WJ*, 4-way junctions. Data are represented as the mean ± S.D.

fork junction (Fig. 4*C*, non-telomeric replication fork with the *inset* showing chickenfoot structure; see also Fig. 4*E*). Protein bound elsewhere on the DNA templates 8 ± 1% of the time. No protein-bound complexes were seen in samples containing DNA and streptavidin alone (data not shown). Intriguingly, the mutant Peptide_M displayed 30 ± 5 and 35 ± 6% binding to the junction and DNA arms of the non-telomeric replication forks, respectively. This reflects an increase in the overall binding from 49% (Peptide_B) to 65% (Peptide_M), with a seemingly small difference in junction binding (41 *versus* 30%, respectively) between the two peptides. However, when we examined the junction binding in more detail, we noticed that the mutant Peptide_M had decreased binding to four-way junctions with little change in binding to three-way junctions (Fig. 4*F*). Specifically, when Peptide_B-bound molecules were evaluated as a fraction of the total DNA molecules with the same shape, Peptide_B bound to 94 ± 9% of all 4-stranded replication fork junctions *versus* 32 ± 8% of all 3-stranded junctions. In contrast, Peptide_M bound to only 33 ± 0% 4-stranded junctions (a reduction in binding of 61%), whereas it was still able to bind to 29 ± 6% of the 3-stranded junctions (a reduction in binding of only 3%). Therefore, it appears that a rearrangement of two conserved amino acids with two non-conserved amino acids disrupted four-way junction binding of the peptide, mimicking the TRF2 basic domain even though overall (nonspecific) binding increased, and binding to the three-way junctions remained largely the same.

The TRF2 truncation mutant, TRF2$^{\Delta B}$, showed only 7 ± 6% binding to the non-telomeric replication fork junctions, preferring to bind somewhere else on the template 26 ± 6% of the time. Therefore, it seems that the loss of the basic domain in the truncated TRF2 construct attenuated its ability to target replication fork junctions, where junction binding was reduced from 48 to 7%, and non-junction binding was increased from 5 to 26% (compare Figs. 3*A* and 4*E*).

These results were more pronounced in EM experiments done with the Holliday junction template (Fig. 4*D*). Junction binding for the Peptide_B, Peptide_M, and TRF2$^{\Delta B}$ constructs was 60 ± 11, 6 ± 4, and 16 ± 6%, respectively, and non-junction binding was 3 ± 1, 22 ± 3, and 12 ± 6% respectively (Fig. 4*E*). Thus, TRF2 binding to the center of Holliday junction templates was reduced by 59% (from 75%) when the basic region was absent, and Peptide_B binding was reduced by 56% (from 60%) in the mutant Peptide_M samples. All of these data suggest, therefore, that the junction binding activity (specifically the four-way junction binding activity) of TRF2 is mediated by the NH_2-terminal amino acids containing the basic domain.

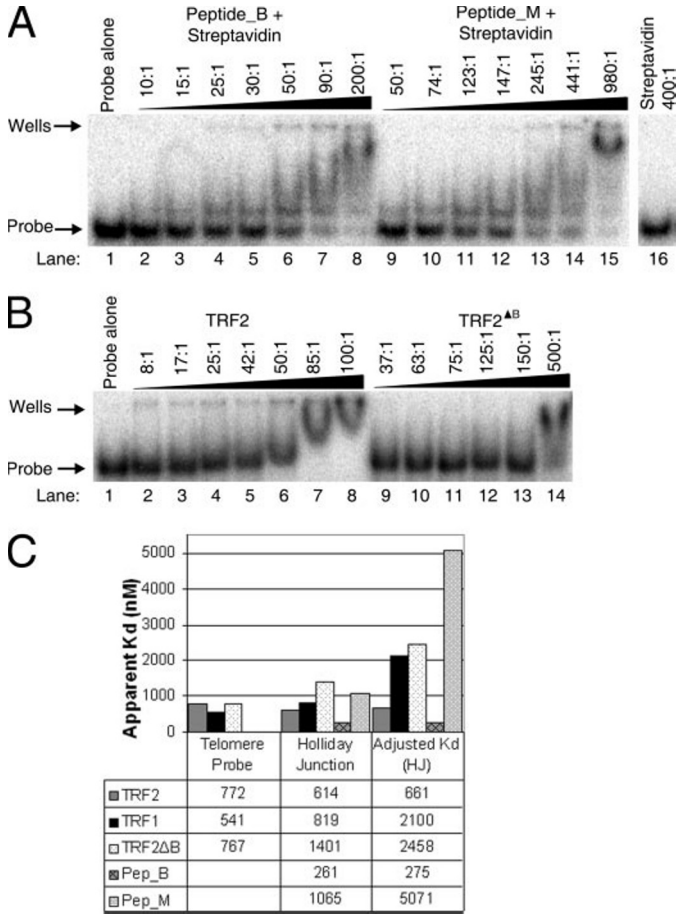

	Telomere Probe	Holliday Junction	Adjusted Kd (HJ)
TRF2	772	614	661
TRF1	541	819	2100
TRF2ΔB	767	1401	2458
Pep_B		261	275
Pep_M		1065	5071

FIGURE 5. **The basic domain of TRF2 is required for binding to four-way junctions.** *A* and *B*, mobility shift assays of the γ-^{32}P-labeled J12 junction probe alone (*lanes 1*) or bound by the basic peptide (*A*, *lanes 2–9*), the mutant peptide (*A*, *lanes 9–15*), streptavidin alone (*A*, *lane 16*); TRF2 (*B*, *lanes 2–8*), and TRF2$^{\Delta B}$ (*B*, *lanes 9–14*). In samples containing peptide, the molar ratio of streptavidin protein:peptide used was 5:1. *C*, apparent dissociation constants (K_d) for TRF2, TRF1, TRF2$^{\Delta B}$, the basic peptide (Pep_B), and the mutant peptide (Pep_M) binding to the small γ-^{32}P end-labeled telomere probe or to the γ-^{32}P end-labeled Holliday junction probe (J12). The last lane (*Adjusted* K_d) shows the apparent K_d values for Holliday junction binding adjusted by the specific binding factors obtained via EM.

To compare the proteins used in this study with respect to Holliday junction binding, mobility shift assays were performed using a constant amount (10 nM) of the small Holliday junction probe in each sample. The concentration was varied for each protein in increasing increments until no more probe could be shifted into the gel. Two examples of these experiments are shown in Figs. 5, *A* and *B*. All experiments were performed a minimum of three times, and averages were taken for each data point. Binding isotherms were generated with % probe shifted (*y* axis) as a function of protein concentration (*x* axis). In all instances, nonlinear regression of the data using a one-site hyperbolic binding equation gave a goodness of fit (R^2) $\geq$ 0.9. The apparent K_d values obtained were, therefore, 614 nM (TRF2), 819 nM (TRF1), 1401 nM (TRF2$^{\Delta B}$), 261 nM (Peptide_B), and 1065 nM (Peptide_M) (Fig. 5*C*). These values may not reflect the true differences in binding, however, because gel-shift analysis does not distinguish junction binding from non-specific dsDNA binding. We, therefore, adjusted the apparent K_d values by the following "specific binding factors" (corresponding to the % junction-specific binding observed for each protein via EM): 93% (TRF2), 39% (TRF1), 57% (TRF2$^{\Delta B}$), 95% (Peptide_B), and 21% (Peptide_M). The resultant *Adjusted* K_d values (Fig. 5*C*) clearly highlight the junction binding of TRF2 (661 nM) sand the basic domain peptide (275 nM) *versus* the more random binding of TRF1 (2100 nM), TRF2$^{\Delta B}$ (2458 nM), and the mutant peptide (5071 nM). Interestingly, the apparent K_d values for TRF1 and TRF2$^{\Delta B}$ are very similar. This result is not surprising considering that both of these proteins have very similar Myb DNA binding domains that would likely bind to non-telomeric DNA with a similar nonspecific affinity.

To test the activity of the telomere-binding proteins under the binding conditions used, the mobility shift binding assays and nonlinear regressions of the data were duplicated using a small γ-^{32}P end-labeled telomeric probe. In all cases, the one-site binding hyperbola again gave a decent fit ($R^2 \geq 0.91$). Binding of all three proteins to the telomeric probe appeared to be equally as good, with TRF1 binding slightly better than the rest (Fig. 5*C*). Most interestingly, TRF2 and TRF2$^{\Delta B}$ had an almost identical affinity for the telomere probe, suggesting that deletion of the basic domain had not destabilized the TRF2 core structure. Therefore, the lower junction binding seen in the TRF2$^{\Delta B}$ constructs appear not to be a result of destabilization of the Myb DNA binding domain. Moreover, under the experimental conditions used, TRF2 appeared to have a slightly smaller K_d when binding to the Holliday junction probe than to the telomeric probe, suggesting that the basic domain of TRF2 has a similar, if not greater, affinity for DNA four-way junctions as the Myb domain has for the consensus telomeric sequence. This was not the case for TRF1 or TRF2$^{\Delta B}$ even before adjusting the K_d values with the EM data. Also, the same mobility shift assays were performed with streptavidin binding to the Holliday junction probe as well as all proteins binding to a small single-stranded DNA probe. In both cases none of the probe was shifted in the gels, indicating the absence of binding (Fig. 5*A*, *lane 16*, and data not shown).

To test the protein domain requirements for TRF2 being able to facilitate t-loop formation *in vitro*, large model telomeres were constructed from a 3.5-kilobase telomere repeat-containing vector such that 560 bp of telomeric repeats were positioned at the end of the linearized DNA. A 54-nucleotide overhang consisting of the sequence TTAGGG$_9$ was ligated onto the end containing the telomere repeats, whereas the opposite end was kept blunt. TRF2 and TRF2$^{\Delta B}$ were simultaneously incubated with the DNA and prepared for EM (9).

TRF2 and TRF2$^{\Delta B}$ appeared to have the same activity and overall affinity for the model telomeres, binding (at all positions) 73 $\pm$ 11% (TRF2) and 68 $\pm$ 15% (TRF2$^{\Delta B}$) of the time, respectively. However, we noticed a difference in the position of each of these proteins on the model telomere template. In experiments containing TRF2, when we considered protein-bound molecules, 50 $\pm$ 10% consisted of a particle of TRF2 bound at the end of the model telomere (Fig. 6, *A* and *E*), and 34 $\pm$ 6% had TRF2 bound within 560 bp of the end of model telomere (presumably within the telomeric repeats). Also observed were molecules where it appeared that the ss over-

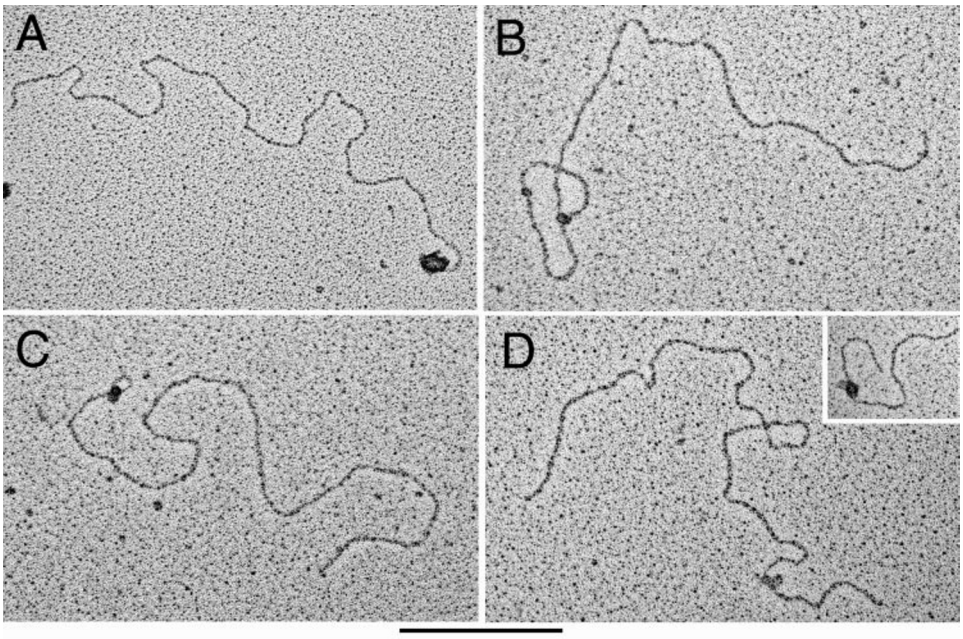

E

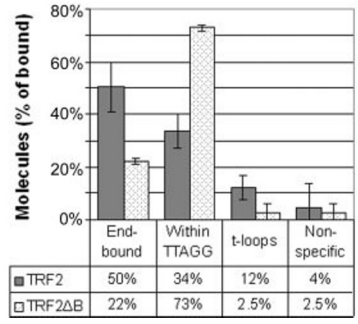

FIGURE 6. **Diminished *in vitro* t-loop formation and telomere ss/ds junction binding by TRF2$^{\Delta B}$.** Binding of TRF2 and TRF2$^{\Delta B}$ to the large model telomeres was visualized by EM and quantified. *A–C*, discrete complexes of TRF2 bound to the ends of the model telomeres (*A*) or at the strand invasion sites of the t-loop (*B* and *C*). *D* and *inset*, TRF2$^{\Delta B}$ typically bound within the TTAGGG repeat tract but not at the ends of the model telomere. The *bar* is equivalent to 450 bp in panels showing full-length molecules. *E*, percentages of molecules with protein bound at the DNA end (end-bound), bound within 560 bp from the end (within TTAGGG), bound at the t-loop invasion site (*t-loops*), or bound more than 560 bp from the DNA end (nonspecific) were calculated as a fraction of all protein-bound molecules scored. Data are represented as mean ± S.D.

hang had invaded the duplex repeat to form a t-loop. Thus, 12 ± 5% of the total protein-bound DNAs consisted of t-loops that had a molecule of TRF2 at the junction of the invasion site (Fig. 6, *B* and *C*). TRF2$^{\Delta B}$ bound to the end of the model telomere in 22 ± 1% of the DNAs, within the telomere repeats 73 ± 1% (Fig. 6*D* and *inset*), and at the junction of a t-loop 2.5 ± 4% of the time. Aggregates of two or more DNAs bound by a large mass of TRF2 or TRF2$^{\Delta B}$ were observed but not scored (data not shown). Our results are, therefore, comparable with previous experiments in our laboratory that were optimized for t-loop formation, where TRF2 bound to t-loop junctions 19% of the time (9). We show, therefore, that the basic domain of TRF2 is involved in t-loop formation on model telomere templates *in vitro*.

DISCUSSION

In this study we used EM and gel-shift assays to evaluate the binding of several telomeric factors to an array of DNA templates. We found that TRF2 was able to bind to the junctions of replication forks, chickenfoot structures, and Holliday junctions, whereas this binding was significantly lower for TRF1 and the TRF2 truncation mutant, TRF2$^{\Delta B}$. TRF2 binding to the DNA junctions did not depend on telomere sequences being present in the DNA, suggesting that the binding was not related to the telomere-specific Myb domain. Also, a bias for four-stranded junctions was observed, especially in non-telomeric substrates, suggesting that these are a major target of TRF2 structure-specific binding.

This raises the question as to whether the three-stranded replication fork junctions that were bound by TRF2 consist of only three DNA strands or might also contain a small extruded fourth (chickenfoot) stem that was not detected by EM. This would be more likely with the telomeric template, where the fork has a natural tendency to regress at repetitive DNAs but is less of a concern with the non-repeat containing replication forks, where spontaneous regression is infrequent and the fraction of chickenfoot intermediates is much lower (1). Also, the fraction of chickenfoot intermediates did not change when TRF2 was added, suggesting that TRF2 was not able to actively regress the fork to produce more stable four-stranded binding substrates (data not shown). Thus, we believe that TRF2 binds to both three-way and four-way DNA junctions *in vitro*.

Of particular interest were the different binding affinities of the two peptides used in this study. The peptide encompassing the basic domain of TRF2 bound well to DNA junctions, with a higher affinity for four-stranded chickenfoot structures than the three-stranded replication fork templates. In contrast, whereas the mutant peptide had the same net charge and amino acid composition of the TRF2 basic domain, binding to four-stranded DNA junctions was greatly disrupted. Thus, the two amino acids, which we rearranged in the mutant peptide and which are conserved within the TRF2 basic domains of some mammals and birds, appear to be important for TRF2 binding to four-way DNA junctions. Although the mutant peptide showed some DNA binding, this likely reflects an electrostatic interaction between the positively charged peptide and negatively charged DNA.

The dissociation constants that were calculated for the proteins binding to radiolabeled Holliday junction probes reflected the stronger affinity of TRF2 and the basic peptide for these templates than TRF1, TRF2$^{\Delta B}$, and the mutant peptide, which all had larger dissociation constants. Also, when

TRF2 binding to large model telomeres was examined by EM, we found that in the absence of the basic domain ($TRF2^{\Delta B}$) the ability of TRF2 to target the end of the large model telomeres was diminished as was its ability to facilitate t-loop formation.

In gel-shift assays with a small telomeric probe, TRF1, TRF2, and $TRF2^{\Delta B}$ all shifted equally as well, with TRF2 and $TRF2^{\Delta B}$ having an almost identical affinity for the telomere probe. Hence, deleting the basic domain from TRF2 does not appear to destabilize the Myb domain, which remained intact in the mutant. The apparent K_d values also suggest that TRF2 DNA-structure binding via the basic domain is equally as strong as telomere-DNA binding via the Myb domain.

The ability of TRF2 to bind telomeric DNA in a sequence-specific manner but to have structure-dependent recruitment to the telomeric ds/ss junction as well as a possible function that is independent of its Myb-dependent binding is reminiscent of the multiple DNA binding properties of p53. p53 has a sequence-specific DNA binding domain as well as an additional domain at its extreme COOH terminus shown to bind in a sequence-nonspecific manner to a wide variety of DNA targets (32, 33, 38). These targets include unusual DNA structures such as the four-stranded DNA Holliday junction, the Y-shaped replication fork, and chickenfoot intermediates of fork regression. Intriguingly, this structure-specific binding domain of p53 is also characterized by basic residues, and it has the same length and overall positive charge as the TRF2 basic domain. We, therefore, consider p53 a good protein to use as a control for *in vitro* binding to DNA junctions, although we do not suggest that these data support a biological role for TRF2 binding to Holliday junctions.

Rather, we infer a biological relevance for TRF2 binding to junctions by considering the $TRF2^{\Delta B}$ phenotype previously studied by Wang *et al.* (11). Deletion of the basic domain did not impede the DNA binding activity of TRF2 nor its localization to telomeres *in vivo*, yet massive losses of telomeric DNA were seen, accompanied by the appearance of telomeric circles, a DNA damage response, and induction of senescence. Moreover, cells expressing the same level of $TRF2^{\Delta B}$ as control cells but with impaired function of XRCC3 protein did not show telomere deletions. We have shown in our laboratory that XRCC3 will bind to Holliday junctions as well as chickenfoot structures *in vitro* in complex with Rad51C.[4] These observations suggest that without the basic domain, TRF2 is unable to protect complex DNA structures at the telomere, such as those that have been seen at model telomere replication forks or the junction structure at the t-loop, from being recognized and processed by DNA repair proteins, including XRCC3. Nevertheless, because $TRF2^{\Delta B}$ is still able to suppress non-homologous end joining events, we believe that the loss of junction binding ability does not directly lead to telomere uncapping, characterized by de-protection and loss of the 3′ overhang, as seen in cells expressing the dominant-negative allele of TRF2 ($TRF2^{\Delta B\Delta M}$) (12).

Based on these findings we suggest a dual role for the TRF2 basic domain at the telomere. The first role involves a critical function during telomere replication in mammals similar to that of Taz1 in the fission yeast (21). We propose that if replication at the telomere stalls because of an impediment to the polymerase machinery, for instance a G-quartet in the unwound G-rich strand, TRF2 would be able to recognize and bind to the chickenfoot intermediates produced by fork regression, thereby preventing the activity of Holliday junction resolvases. TRF2 can then recruit factors like the RecQ helicases to unwind the chickenfoot structures, allowing replication to restart. Indeed, this may explain why TRF2 is able to interact with and stimulate the RecQ helicases, known to be important for proper telomere replication and maintenance in human cells (28, 29). The second role for TRF2 involving the basic domain would be a role for TRF2 in t-loop formation and stabilization. We propose that the junction binding property of the basic domain enhances the ability of TRF2, in conjunction with other telomere-associated proteins, to target chromosome ends and facilitate t-loop formation. Junction binding capacity would also make it possible for TRF2 to contribute to the stability of the t-loop by binding to junctions formed at the strand invasion site of the t-loop.

We previously observed that psoralen cross-linking stabilized t-loop formation *in vitro* on DNAs with very short overhangs, suggesting that more than just the nucleotides of the ss tail are inserted into the duplex to form the D-loop (9). Based on our findings we would further suggest that the more energetically favorable structure at the strand invasion site is a four-way junction (preferred by TRF2 to the three-way junction) formed by branch migration of the invasion site. The data are also the first direct demonstration of TRF2 binding specifically and selectively to non-telomeric DNA *in vitro* and may explain the ability of TRF2 to localize to sites of DNA damage in irradiated human fibroblasts (13).

Acknowledgments—We thank Dr. Titia de Lange (The Rockefeller University, New York) for the generous donation of the $TRF2^{\Delta B}$ baculovirus and Dr. Brenda R. S. Temple (Structural Bioinformatics Core Facility, University of North Carolina) for critical discussions and help with the mutant peptide design.

[4] S. Compton, unpublished results.

REFERENCES

1. Fouché, N., Özgür, S., Roy, D., and Griffith, J. (2006) *Nucleic Acids Res.*, in press
2. Moyzis, R. K., Buckingham, J. M., Cram, L. S., Dani, M., Deaven, L. L., Jones, M. D., Meyne, J., Ratliff, R. L., and Wu, J. R. (1988) *Proc. Natl. Acad. Sci. U. S. A.* **85,** 6622–6626
3. Henderson, E. R., and Blackburn, E. H. (1989) *Mol. Cell Biol.* **9,** 345–348
4. Griffith, J. D., Comeau, L., Rosenfield, S., Stansel, R. M., Bianchi, A., Moss, H., and de Lange, T. (1999) *Cell* **97,** 503–514
5. de Lange, T. (2005) *Genes Dev.* **19,** 2100–2110
6. Lansdorp, P. M. (2005) *Trends Biochem. Sci.* **30,** 388–395
7. de Lange, T. (2002) *Oncogene* **21,** 532–540
8. Griffith, J., Bianchi, A., and de Lange, T. (1998) *J. Mol. Biol.* **278,** 79–88
9. Stansel, R. M., de Lange, T., and Griffith, J. D. (2001) *EMBO J.* **20,** 5532–5540
10. Broccoli, D., Smogorzewska, A., Chong, L., and de Lange, T. (1997) *Nat. Genet.* **17,** 231–235
11. Wang, R. C., Smogorzewska, A., and de Lange, T. (2004) *Cell* **119,** 355–368
12. van Steensel, B., Smogorzewska, A., and de Lange, T. (1998) *Cell* **92,** 401–413

13. Bradshaw, P. S., Stavropoulos, D. J., and Meyn, M. S. (2005) *Nat. Genet.* **37,** 193–197
14. Greider, C. W. (1996) *Annu. Rev. Biochem.* **65,** 337–365
15. Greider, C. W., and Blackburn, E. H. (1987) *Cell* **51,** 887–898
16. Diede, S. J., and Gottschling, D. E. (1999) *Cell* **99,** 723–733
17. Ohki, R., and Ishikawa, F. (2004) *Nucleic Acids Res.* **32,** 1627–1637
18. Wang, Y., and Patel, D. J. (1993) *Structure* **1,** 263–282
19. Phan, A. T., Gueron, M., and Leroy, J. L. (2000) *J. Mol. Biol.* **299,** 123–144
20. Ten Hagen, K. G., Gilbert, D. M., Willard, H. F., and Cohen, S. N. (1990) *Mol. Cell. Biol.* **10,** 6348–6355
21. Miller, K. M., Rog, O., and Cooper, J. P. (2006) *Nature* **440,** 824–828
22. Crabbe, L., Verdun, R. E., Haggblom, C. I., and Karlseder, J. (2004) *Science* **306,** 1951–1953
23. Lillard-Wetherell, K., Machwe, A., Langland, G. T., Combs, K. A., Behbehani, G. K., Schonberg, S. A., German, J., Turchi, J. J., Orren, D. K., and Groden, J. (2004) *Hum. Mol. Genet.* **13,** 1919–1932
24. Bai, Y., and Murnane, J. P. (2003) *Hum. Genet.* **113,** 337–347
25. Yang, Q., Zhang, R., Wang, X. W., Spillare, E. A., Linke, S. P., Subramanian, D., Griffith, J. D., Li, J. L., Hickson, I. D., Shen, J. C., Loeb, L. A., Mazur, S. J., Appella, E., Brosh, R. M., Jr., Karmakar, P., Bohr, V. A., and Harris, C. C. (2002) *J. Biol. Chem.* **277,** 31980–31987
26. Constantinou, A., Tarsounas, M., Karow, J. K., Brosh, R. M., Bohr, V. A., Hickson, I. D., and West, S. C. (2000) *EMBO Rep.* **1,** 80–84
27. Karow, J. K., Constantinou, A., Li, J. L., West, S. C., and Hickson, I. D. (2000) *Proc. Natl. Acad. Sci. U. S. A.* **97,** 6504–6508
28. Machwe, A., Xiao, L., and Orren, D. K. (2004) *Oncogene* **23,** 149–156
29. Opresko, P. L., von Kobbe, C., Laine, J. P., Harrigan, J., Hickson, I. D., and Bohr, V. A. (2002) *J. Biol. Chem.* **277,** 41110–41119
30. Opresko, P. L., Mason, P. A., Podell, E. R., Lei, M., Hickson, I. D., Cech, T. R., and Bohr, V. A. (2005) *J. Biol. Chem.* **280,** 32069–32080
31. Opresko, P. L., Otterlei, M., Graakjaer, J., Bruheim, P., Dawut, L., Kolvraa, S., May, A., Seidman, M. M., and Bohr, V. A. (2004) *Mol. Cell* **14,** 763–774
32. Subramanian, D., and Griffith, J. D. (2005) *J. Biol. Chem.* **280,** 42568–42572
33. Lee, S., Cavallo, L., and Griffith, J. (1997) *J. Biol. Chem.* **272,** 7532–7539
34. Alani, E., Lee, S., Kane, M. F., Griffith, J., and Kolodner, R. D. (1997) *J. Mol. Biol.* **265,** 289–301
35. Bianchi, A., Smith, S., Chong, L., Elias, P., and de Lange, T. (1997) *EMBO J.* **16,** 1785–1794
36. Wu, L., Bayle, J. H., Elenbaas, B., Pavletich, N. P., and Levine, A. J. (1995) *Mol. Cell. Biol.* **15,** 497–504
37. Griffith, J. D., and Christiansen, G. (1978) *Annu. Rev. Biophys. Bioeng.* **7,** 19–35
38. Lee, S., Elenbaas, B., Levine, A., and Griffith, J. (1995) *Cell* **81,** 1013–1020